Fractal dimensions of electronic wavefunctions for a tight-binding model on the Fibonacci chain.

Nicolas Macé, Anuradha Jagannathan, and Frédéric Piéchon

Laboratoire de physique des Solides, Université Paris-Saclay, 91400 Orsay, France

(Dated: May 22, 2015)

Abstract

INTRODUCTION

We focus on tight-binding Hamiltonians on one-dimensional quasiperiodic tilings. Notable examples include the Harper model, and the family of quasiperiodic Hamiltonians constructed by the cut and project method. Each of the latter is associated with an irrational number, α. It has the geometrical interpretation of the tangent of the angle between the projection axis and the direction of one of the basis vectors of the two-dimensional superlattice. The Hamiltonian of such a model writes

$$H^\alpha = \sum_i t_i^\alpha \left(|i\rangle \langle i+1| + |i+1\rangle \langle i| \right) \tag{1}$$

where the jump amplitudes t_i^α can take two values t_s, t_w:

$$t_i^\alpha = \begin{cases} t_w & \text{when } i \bmod (1+\alpha) \geq \alpha, \\ t_s & \text{otherwise.} \end{cases} \tag{2}$$

If we replace the irrational α by a rational approximation $\alpha_n = p_n/q_n$, the sequence of couplings is modified:

$$t_i^{p_n/q_n} = \begin{cases} t_w & \text{when } q_n i \bmod (p_n+q_n) \geq p_n, \\ t_s & \text{otherwise,} \end{cases} \tag{3}$$

and we obtain a periodic system of period p_n+q_n. Thus, to a sequence of rationals $\{\alpha_n\}_n$ converging to α is associated in a natural way a sequence of periodic tight-binding Hamiltonians – called approximants, converging to a quasiperidic Hamiltonian. We will call H_n the n^{th} approximant, generated by the rationnal α_n.

Amongst all irrationals, the golden ratio and its inverse, $\omega = 2/(1+\sqrt{5})$, play a special role. They contain only the number 1 in their continued fraction expansion. In that sense, these two numbers are the hardest to approximate by rationnals. We thus expect the quasiperiodicity to have the most spectacular consequences when the irrational is taken to be the golden ratio or its inverse.

We restrict ourselves to the case $\alpha \leq 1$ (the other case being equivalent up the exchange of t_s and t_w). As an example, we are going to chose $\alpha = \omega$. The tight-binding Hamiltonian resulting from this choice is called the Fibonacci Hamiltonian. However, our results are general and apply to every Hamiltonian constructed by the cut and project method.

CO-NUMBERING, ATOMS AND MOLECULES.

We consider a periodic approximant given by the rational $\alpha_n = p_n/q_n$. Later, we are going to specialize to the case of the Fibonacci Hamiltonian, but for the moment we wish to stay as general as possible. We have already seen already that the integer

$$i'_k = q_n k \bmod (p_n + q_n) \tag{4}$$

determines the sequence of jump amplitudes. How does i'_k changes when we jump from one site to the next, i.e. when we increase k by one unit? It is easy to check that

$$i'_{k+1} = \begin{cases} i'_k - p_n & \text{when sites } k \text{ and } k+1 \text{ are linked by } t_w, \\ i'_k + q_n & \text{when sites } k \text{ and } k+1 \text{ are linked by } t_s. \end{cases} \tag{5}$$

Thus, the sequence of i'_k furnishes a natural renumbering of the sites, as was first noted by R. Mosseri [5]. A generalization of this renumbering to higher dimensional quasicrystals can be found in [8]. In the basis where sites are numbered using i', up to a suitable shift of the origin, the Hamiltonian rewrites as a two-banded Toeplitz matrix:

$$H_n = \begin{array}{c} \\ 1 \\ \vdots \\ p_n \\ \vdots \\ q_n \\ \vdots \end{array} \begin{array}{c} \begin{array}{ccccccccccc} 1 & \dots & & p_n & & \dots & & q_n & & \dots \end{array} \\ \begin{pmatrix} 0 & \dots & 0 & t_w & 0 & \dots & 0 & t_s & 0 & \dots \\ & & & & \ddots & & & & \ddots & \\ t_w & & & & & & & & & \\ & \ddots & & & & & & & & \\ t_s & & & & & & & & & \\ & \ddots & & & & & & & & \\ & & & & & & & & & \end{pmatrix} \end{array} \tag{6}$$

The co-numbering allows to distinguish two classes of sites. We call *molecular* the first p_n and the last p_n sites. We call *atomic* the remaining $q_n - p_n$ sites. Each molecular site is coupled to another molecular site by a t_s coupling, and to an atomic site by a t_w coupling. Thus, in the limit $t_w \ll t_s$, molecular sites form isolated diamtomic *molecules*. On the other hand, the atomic sites are all coupled to two molecular sites by t_w couplings. Thus, in the limit $t_w \ll t_s$, they form isolated *atoms*.

Now, we focus on the particular case of the Fibonacci Hamiltonian. We take $p_n = F_{n-2}$, $q_n = F_{n-1}$ where F_n is the n^{th} Fibonacci number. Then, $\alpha_n = F_{n-2}/F_{n-1}$ indeed approximates the inverse golden ratio, so that we have constructed an approximant to the Fibonacci chain. The n^{th}

Fibonacci approximant consists of a block of $F_{n-2} + F_{n-1} = F_n$ sites, repeated periodically. That block contain $F_{n-1} - F_{n-2} = F_{n-3}$ atoms and F_{n-2} molecules (that is, $2F_{n-2}$ molecular sites).

Figure (1) shows the molecules and atoms of the fifth Fibonacci approximant, together with the co-numbering of the sites.

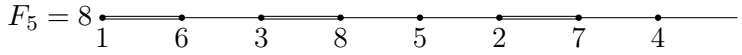

Figure 1: The periodically repeated block of the fifth approximant to the Fibonacci chain. Weak couplings t_w are represented by a single line, and strong couplings t_s by a double line. Below each site is its co-numbered label.

DEFLATION AND RENORMALIZATION

Deflation, molecular and atomic chains.

Besides the cut and project method, we can construct the Fibonacci chain by inflation. We start from the trivial chain:

$$C_0 = t_s \tag{7}$$

and we apply repetively the *inflation rule*

$$r \stackrel{\text{def}}{=} \begin{cases} t_w & \to t_w t_s \\ t_s & \to t_w \end{cases} \tag{8}$$

on it to build new chains: $C_1 = r(C_0) = t_w$, $C_2 = r(C_1) = t_w t_s$, ... $C_n = r^n(C_0)$. Then, perhaps up to a global circular permutation of the couplings, the infinite chain $C_n C_n C_n \dots$ is the sequence of couplings of the n^{th} approximant. Furthermore, we can define *deflation rules* relating an approximant to a smaller one. The *molecular deflation rule*

$$d_m = \begin{cases} t_w & \leftarrow t_s t_w t_w (t_s) \\ t_s & \leftarrow t_s t_w (t_s) \end{cases} \tag{9}$$

decimates all sites except molecular ones. Fig. (2) examplifies the decimation operation. Crucially, the deflated chain is again a Fibonacci chain. More precisely, the molecular deflation relates the approximant of size n to the approximant of size $n-2$: $d_m(C_n C_n \dots) = C_{n-2} C_{n-2} \dots$.

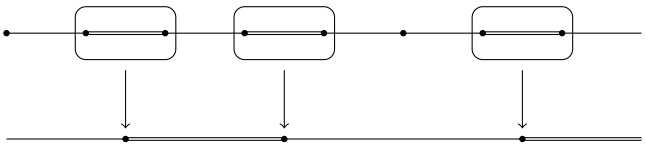

Figure 2: The molecular deflation rule illustrated. Here we relate the fifth approximant to the third.

Similarly, we can perform a decimation operation on all sites except atomic ones. We call such an operation an *atomic decimation*. Again, the deflated chain is also a Fibonacci chain. The atomic decimation relates the approximant of size n to the approximant of size $n-3$. Fig. (3) examplifies the procedure.

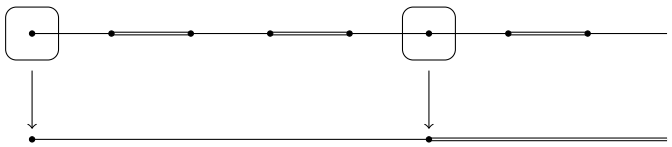

Figure 3: The atomic deflation rule illustrated. Here we relate the fifth approximant to the second.

Renormalization

We are now going to focus on the limit $t_w \ll t_s$, in which the disinction between atomic and molecular sites acquires its real meaning. We define $\rho = t_w/t_s$. It will be our perturbative parameter. The energies are at most of order t_s. As varying t_s (while keeping ρ fixed) simply amounts to rescaling the whole energy spectrum, we arbitrarily set $t_s = 1$.

When $\rho = 0$, the atoms and the molecules decouple. The eigenstates are the molecular bonding and antibonding states, at energies ± 1, and the atomic state at zero energy. The spectrum is constituted of three infinitely degenerated levels.

When $\rho > 0$, $\rho \ll 1$, perturbation theory tells us that states inside each of the three degenerated levels weakly coupled to each other, thus raising the degeneracy. Let us focus to begin with on atomic states. At first order, each atomic site is coupled to the neighbouring atomic sites. Effectively, we can therefore work on the *deflated* chain, with effective hopping amplitudes coupling atomic sites. Perturbation theory gives us the expression of the effective hopping amplitudes [6].

We find

$$\begin{cases} t_w^{\text{atomic}} &= \overline{z}\rho \\ t_s^{\text{atomic}} &= \overline{z}, \end{cases} \tag{10}$$

with $\overline{z} = \rho^2$.

Similarly, each molecular site is coupled to the neighbouring molecular sites. There is here a small subtlety. A molecule sits on two neighbouring sites. Say for example that that sites i and $i+1$ on the chain form a molecule. Then, by a change of basis, we can say that the molecule sits at the "bonding" and "antibonding" *effective* sites respectively given by the linear combination of the localized states $|i\rangle + |i+1\rangle$ and $|i\rangle - |i+1\rangle$. It is natural to do that, because when $\rho = 0$ the molecular eigenstates are localized in this new basis. At first order, the bonding sites of neighbouring molecules couple to each other. This results in effective hopping amplitudes given by

$$\begin{cases} t_w^{\text{bonding}} &= z\rho \\ t_s^{\text{bonding}} &= z, \end{cases} \tag{11}$$

with $z = \rho/2$. This also results in the appearance of an onsite potential, $V^{\text{bonding}} = -1$. The antibonding sites similarly couple to each other, resulting in the same effective hopping terms, but in a different onsite potential, $V^{\text{antibonding}} = +1$.

To summarize, we have seen that we can formally separate the chain of the n^{th} approximant into molecular and atomic chains. In the limit $\rho \ll 1$, the Hamiltonian of the n^{th} approximant decouples into the direct sum of three Hamiltonians: an atomic Hamiltonian living on the chain formed of atomic sites, a bonding Hamiltonian living on the chain formed of molecular bonding sites, and an antibonding Hamiltonian living on the chain formed of molecular antibonding sites. Because the atomic and molecular chains are again Fibonacci chains (but of smaller lengths), these three Hamiltonians are Fibonacci Hamiltonians, with renormalized hopping terms and onsite energies. Formally, we have:

$$H_n = \underbrace{(zH_{n-2} - 1)}_{\text{bonding sites}} \oplus \underbrace{(\overline{z}H_{n-3})}_{\text{atomic sites}} \oplus \underbrace{(zH_{n-2} + 1)}_{\text{antibonding sites}} + \mathcal{O}(\rho^4) \tag{12}$$

In the limit $n \to \infty$, the chain becomes quasiperiodic. As such, we expect its wavefunctions and its spectrum to be nontrivial, namely to exhibit multifractality. We are going to try using the recursion relation we have on the Hamiltonians of the approximants to derive recursion relations on energies and wavefunctions. In this way, we hope to gain some insight on the form of the spectrum and of the wavefunctions in the limit $n \to \infty$. From that, we hope to characterize the

multifractality of the quasiperiodic chain by computing the fractal dimensions of its wavefunctions and of its spectrum.

Renormalization paths, equivalence between energy labels and co-numbers.

Since the Hamiltonian of an approximant is the direct sum of three Hamiltonians, the energy spectrum can be expressed as the union of three spectra. Specifically, the spectrum $\mathcal{S}_n$ of the n^{th} approximant is the union of scaled version of the spectra at step $n-2$ and $n-3$:

$$\mathcal{S}_n = (z\mathcal{S}_{n-2} - 1) \bigcup (\overline{z}\mathcal{S}_{n-3}) \bigcup (z\mathcal{S}_{n-2} + 1) \tag{13}$$

So, we can distinguish between three energy clusters: the antibonding molecular energy cluster, the atomic energy cluster and the bonding energy cluster. Molecular clusters are separated from the atomic cluster by a gap of width $\Delta \sim 1 - z$.

Relation (13) tells us that each of these three clusters is the spectrum of a smaller approximant, and as such, it decomposes in its turn into three bands, etc. The spectrum has therefore a recursive, Cantor set-like description.

This has an important consequence: we can associate to a given energy level of the n^{th} approximant a unique sequence of labels called its *renormalization path* in the following way. If it is in the upper band, associated to molecular bounding states, we give it a + label. If it is in the middle band, associated to atomic states, we give it a 0 label, and if it is in the lower band , associated to molecular antibonding states we give it a − label. But then, the cluster our energy level belongs to is again the spectrum of some approximant (of size $n-2$ if it is the upper or lower band, of size $n-3$ if it is the middle band). We can thus repeat this labelling procedure recursively, and indeed assign to each energy level of the n^{th} approximant a unique sequence of labels, its renormalization path. We can plot these sequences on a trifurcating tree (fig. (4)), as was already pointed out [3] [7].

We can also associate to a given site of the n^{th} approximant a unique renormalization path in the following way. If it is an antibonding site, we give it a + label. If it is an atomic site, we give it a 0 label, and if it is a bonding site we give it a − label. But then, the family (bonding, antibonding or atomic) our site belongs to forms again a Fibonacci chain (of size $n-2$ for bonding and antibonding sites, of size $n-3$ for atomic sites). Thus, as for energy levels, we can repeat this labelling procedure recursively, and indeed assign to each site of the n^{th} approximant a unique renormalization path.

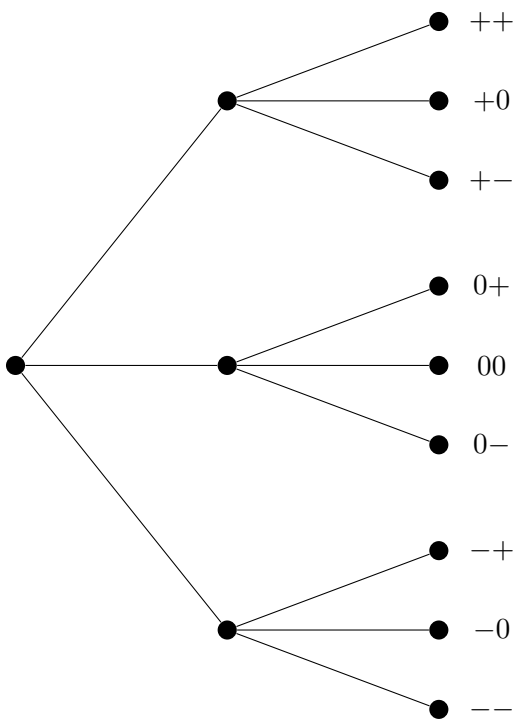

Figure 4: Trifurcating tree of energies. Each dot symbolizes an energy level. To the right of the deepest energy levels is written their renormalization path.

Now, we want to characterize completely the eigenstates of the n^{th} approximant. Given an energy level, we consider the associated eigenstate. Equation (12) tells us that at leading order in ρ, the eigenstate has nonzero amplitude only on molecular bonding sites, on atomic sites or on antibonding sites if it associated respectively to an energy in the bonding, in the atomic or in the antibonding energy cluster. In other words, the eigenstate has nonzero amplitude on a site only if the first letter of its renormalization path is the first lettter of the renormalization path of the energy level of the eigenstate. We can repeat this reasoning recursively, and we conclude that *the eigenstate has a nonzero amplitude only on sites whose renormalization path matches the one of the energy level.*

In conclusion, we have completely characterized the eigenstates of the n^{th} approximant, and in the course of doing so, we have proved the equivalence between renormalization paths of sites and of energy levels. To render this equivalence more obvious and visual, we can employ the conumbering of sites. In conumbering, the first and the last F_{n-2} sites of the n^{th} approximant are molecular (bonding or antibonding) sites, while the remaining F_{n-3} middle sites are atomic. We can repeat this reasoning recursively: amongst the first F_{n-2} sites, the first and last F_{n-4} sites are molecular at step $n-2$, etc. Thus, in conumbering, sites are naturally ordered by their

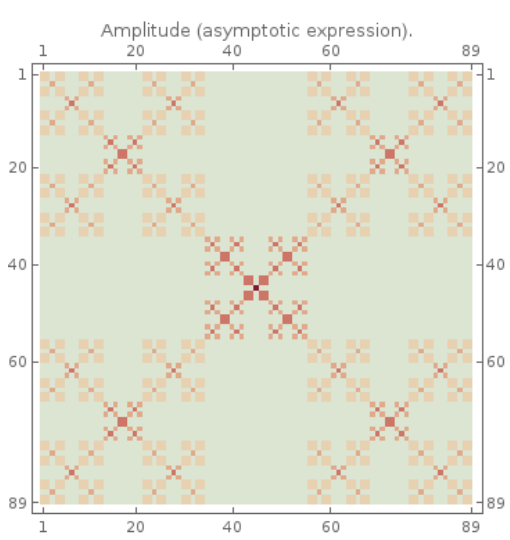

(a) LDoS, asymptoptic expression.

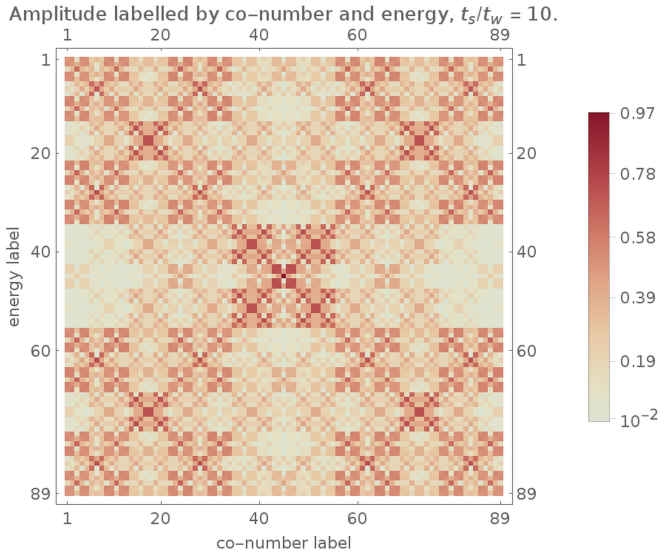

(b) LDoS, numerical expression.

Figure 5: The local density of states, as a function of the position label (in conumbering), and of the energy label, for the eigth approximant constituted of 89 sites.

renormalization path, and the ordering is exactly the same as the one of the energy levels. So, plotting the local density of states as a function of the energy label and the site conumber, should make obvious the equivalence between renormalization paths of sites and of energy levels. More precisely, the local density of states should be left invariant under the exchange of the site label and the energy label axes. This is indeed what we observe, both analytically (5a) and numerically for small values of ρ (5b).

Now that we have completely characterized the spectrum and the wavefunction to leading order in ρ, we can derive from that expressions for the fractal dimensions of the spectrum and of the wavefunctions.

FRACTAL DIMENSIONS AT LEADING ORDER

Fractal dimensions of the spectrum

We compute the fractal dimensions of the spectrum using the thermodynamical formalism [2]. We define the partition function

$$\Gamma^n(q,\tau) = \sum_a \frac{(1/F_n)^q}{(\Delta_a^n)^\tau} \tag{14}$$

where Δ_a^n is taken to be the width of the energy band associated to the energy level labeled a. One can show [2] that the generalized fractal dimensions of the spectrum D_q are given by $D_q = \tau_q/(q-1)$ where τ_q is defined by

$$\Gamma^n(q, \tau > \tau_q) \to +\infty \tag{15}$$

$$\Gamma^n(a, \tau < \tau_q) \to 0 \tag{16}$$

In practice, a good approximation of τ_q is given by $\Gamma^{n+1}(q, \tau_q)/\Gamma^n(q, \tau_q) = 1$ for n large.

In particular, the Hausdorff dimension, D_0, helps characterizing the nature of the spectrum. $D_0 = 0$ for a pure-point spectrum, while $D_0 = 1$ indicates that the spectrum has an absolutely continuous component. An intermediate value $0 < D_0 < 1$ is the signature of a fractal spectrum, whose multifractal properties can be probed by varying q.

At leading order, the recursion relation between energies (13) translates into a recursion relation between partition functions. This makes it easy to find the fractal dimensions of the spectrum [7] *via* the implicit equation

$$2\omega^{2q} z^{-(q-1)D_q} + \omega^{3q} \overline{z}^{-(q-1)D_q} = 1. \tag{17}$$

Thus, we have

$$D_q = \frac{1}{1-q} \frac{\log\left[\omega^{-q}\left(\sqrt{1+\omega^{-q}} - 1\right)\right]}{\log \rho} + \mathcal{O}\left(\frac{1}{(\log \rho)^2}\right) \tag{18}$$

In particular, we find for the Hausdorff dimension

$$D_0 = \frac{\log(\sqrt{2}-1)}{\log \rho} + \mathcal{O}\left(\frac{1}{(\log \rho)^2}\right) \tag{19}$$

in agreement with the result of Damanik & Gorodetski [1], using trace-map-based methods.

We have $0 < D_0 < 1$ for $\rho > 0$. Therefore we recover the well-established result that the spectrum of the Fibonacci hamiltonian is fractal as soon as $\rho > 0$.

Fractal dimensions of the wavefunctions

The fractal dimensions $D_q^\psi(a)$ of the wavefunction associated to the energy level a are defined by

$$\chi_q^n(a) = \sum_i |\psi_i^n(a)|^{2q} \underset{n\to\infty}{\sim} \left(\frac{1}{F_n}\right)^{(q-1)D_q^\psi(a)} \tag{20}$$

Note that $D_2^\psi(a)$ is the inverse participation ratio. $D_2^\psi(a) = 1$ indicates that the state a is extended, while $D_2^\psi(a) = 0$ characterizes a localized state. An intermediate value $0 < D_2^\psi(a) < 1$ is the signature of a critical state, whose multifractal properties can be probed by varying q.

At leading order in ρ the renormalization of the eigenstates is trivial. On a site whose renormalization path matches the one of the energy level we consider, the amplitude at step n is just the amplitude at step $n-3$ if the energy is in the atomic cluster, while the amplitude is the one at step $n-2$ divided by a factor $\sqrt{2}$ if the energy is in the molecular cluster. The division by a factor of $\sqrt{2}$ simply comes from the fact that molecular sites are in pairs.

Therefore, we have for the fractal dimensions of the wavefunction of the energy level labeled by a,

$$D_q^\psi(a) = x_a \frac{\log 2}{\log \omega^{-1}} + \mathcal{O}(\rho^2), \tag{21}$$

where

$$x_a = \lim_{n\to\infty} \frac{n_+(a) + n_-(a)}{n} \tag{22}$$

with $n_\pm(a)$ the number of $+/-$ letters in the renormalization path of a. In other words, x_a is the fraction of renormalization steps in which the level a was in a molecular cluster.

Since $x_a \leq 1/2$, we have $0 < D_q^\psi(a) < 1$: the wavefunctions are critical, as we expect for a quasiperiodic system. We have $x_a = 0$ for the level that has the renormalization path 00..., ie for the energy level $E = 0$, at the center of the atomic cluster. The corresponding eigenstate has a zero fractal dimension, and is thus completely localized. As we approach the $E = 0$ level, x_a approaches monotonously 0 and the wavefunctions becomes more and more localized. x_a reaches its maximal value, $1/2$, for the levels having the renormalization path $++...$ and $--...$, ie for the levels $E = E_{\min}, E_{\max} = \pm 1/(1+z)$ at the edges of the spectrum. The corresponding eigenstates are the most extended. They occupy a fraction $(1/F_n)^{\frac{\log 2}{\log \omega^{-2}}}$ of the sites.

It is also interesting to note that the fractal dimensions of the wavefunction does not depend on q: the wavefunctions are not multifractal. We expect multifractality to appear at the next-to-leading order in ρ. To go beyond the leading order – where the interesting physics lies! – we have to consider overlap between atoms and molecules.

FRACTAL DIMENSIONS AT NEXT-TO-LEADING ORDER AND MULTIFRACTALITY

At next-to-leading order the picture of molecular and atomic eigenstates and energies remains relevant, but it is now possible for an atomic eigenstate to have nonzero amplitude on molecular sites, and vice-versa. A complete analysis of the situation would require pushing perturbation theory to the next order. However, as long as we are interested in computing fractal dimensions, we only need to know the corrections to the wavefunction amplitudes at the sites where they had

nonzero amplitude at leading order.

It is easier to encode the corrections to leading order in a multiplicative factor:

$$\psi_i^n(a) = \sqrt{\lambda_i(a)}\psi_i^{n,(0)}(a), \tag{23}$$

where $\psi^{(0)}$ is the wavefunction at leading order. This is more than a simple formal rewriting of the expansion of the wavefunction around $\rho = 0$. Indeed, $\psi_i^{n,(0)}(a)$ is related by the renormalization group to a wavefunction coefficient of a smaller approximant. specifically we have $\psi_i^{n,(0)}(a) = \psi_{i'}^{n-3,(0)}(a')$ for an energy of the atomic cluster, and $\psi_i^{n,(0)}(a) = \psi_{i'}^{n-2,(0)}(a')/\sqrt{2}$ for an energy of the molecular clusters. Thus, $\lambda_i(a)$ has the meaning of the correction to the renormalization of the wavefunctions, appearing when we take into account higher order terms in ρ.

We call $\lambda(a)$ the average of $\lambda_i(a)$ over all sites, at fixed energy E_a. We can formally write

$$\lambda_i(a) = \lambda(a) + \Delta\lambda_i(a). \tag{24}$$

Numerically, we observe that the fluctuations are negligible relative to the mean value. More precisely, we have

$$\lambda(a)^q \gg \lambda(a)^{q-k}\Delta\lambda_i(a)^k, \ \forall k \in [1, q] \tag{25}$$

The validity of the approximation improves as q becomes larger.

This means that, for $q \geq 1$, we can write

$$\chi_q^n(a) = \begin{cases} \lambda(a)^q \chi_q^{n-3}(a') & \text{if } a \text{ is an atomic level,} \\ (\lambda(a)/2)^q \, \chi_q^{n-2}(a') & \text{if } a \text{ is a molecular level.} \end{cases} \tag{26}$$

Iterating this recurrence relation, we find that

$$\chi_q^n(a) = (\lambda(a)\lambda(a')...)^q \, \chi_q^{n,(0)}(a). \tag{27}$$

The product $\lambda(a)\lambda(a')...$ encodes the next-to-leading order corrections to χ. It depends only on the sequence $a, a', ...$ that the energy level a follows under the action of the renormalization group. Said differently, the corrections to χ, and therefore the fractal dimensions, depend only on the renormalization path of the level a.

We make the further approximation – again supported by numerical evidences – that the renormalization factor $\lambda(a)$ is constant over the atomic and the molecular clusters:

$$\lambda(a) = \begin{cases} \overline{\lambda} & \text{if } a \text{ is an atomic level,} \\ \lambda & \text{if } a \text{ is a molecular level.} \end{cases} \tag{28}$$

We are able to compute $\overline{\lambda}$ and λ (see the appendix () for the details). We find

$$\begin{cases} \overline{\lambda} = 1/(1+2\rho^2) + \mathcal{O}(\rho^4), \\ \lambda = 1/(1+\rho^2/2) + \mathcal{O}(\rho^4). \end{cases} \tag{29}$$

Furthermore, we are able to solve the reccurence relation (27) completely. We find

$$D_q^{\psi}(a) = D_q^{\psi,(0)}(a) - \frac{q}{q-1}\left(x_a \frac{\log\lambda}{\log\omega^{-1}} + \frac{1-2x_a}{3}\frac{\log\overline{\lambda}}{\log\omega^{-1}} \right). \tag{30}$$

Note that this result is indenpendant of the specific values of $\overline{\lambda}$ and λ. Plugging in the values (29), we get

$$D_q^{\psi}(a) = D_q^{\psi,(0)}(a) + \frac{q}{q-1}\frac{4-5x}{6}\frac{\rho^2}{\log\omega^{-1}} + \mathcal{O}(\rho^4). \tag{31}$$

Indeed, the next-to-leading order corrections are q-dependant: they encode the multifractality of the wavefunctions.

We now check our theoretical predictions against numerical results.

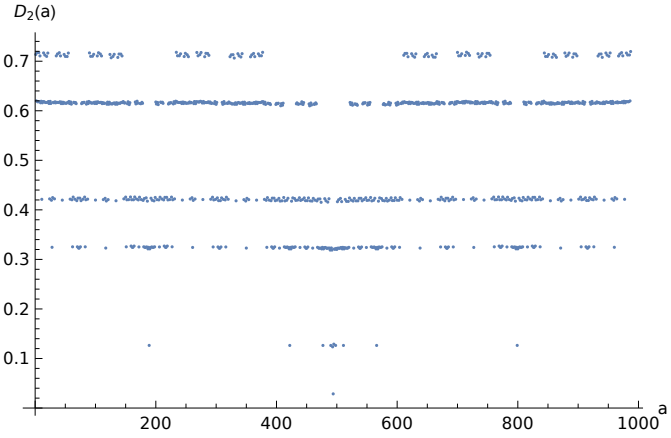

(a) The fractal dimension $D_2^{\psi}(a)$ for every wavefunction. In accordance with theoretical predictions, the fractal dimensions organize in lines, each line corresponding to a given value of x_a.

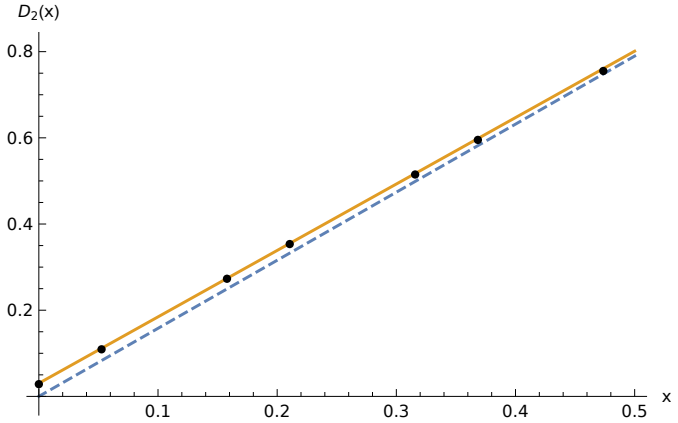

(b) Dots: fractal dimension $D_2^{\psi}(a)$ averaged over states a having a given x_a. Dashed line: theoretical prediction at leading order (eq. (21)). Solid line: theoretical prediction including multifractal corrections (eq. (31)).

Figure 6: Numerical results and theoretical predictions for the fractal dimensions of the wavefunctions, in the $\rho \to 0$ limit. Numerically we took $\rho = 1/10$, and worked on the approximant $n = 19$ (4181 sites). On figure (6a) we chose the approximant $n = 16$ for the sake of clarity.

Figure (6a) shows how the fractal dimension for a given q (here we chose abitrarily $q = 2$) depend on the the chosen state a. we observe that the value of the fractal dimension organizes in lines. On each line $D_q^\psi(a)$ is constant up to small variations. Moreover, a given line is formed of all the points $(a, D_q^\psi(a))$ having a given value $x_a = x$. So, we conclude that, up to small variations that should vanish in the limit $\rho \to 0$, the fractal dimension of a given wavefunction does not depend on the associated state a, but only on x_a. This is in agreement with the theoretical predictions (31).

It is therefore meaningful to compute numerically the fractal dimensions averaged over each state a having a given x_a value. We thus obtain the fractal dimensions as a function of the relevant parameter, x. Figure (6b) shows the x dependance of the fractal dimension for $q = 2$. The numerical results are in good agreement with the theoretical predictions. Most interestingly, we see that taking into account the next-to-leading order corrections is required to obtain a good agreement with the numerical results. So indeed, the multifractal properties of the wavefunctions – wich are not captured at leading order in ρ – are relevant, even for fairly small couplings ($\rho \sim 1/10$). As fig. (6b) shows, the multifractal corrections are most relevant for $x \to 0$. This is easily understandable: for $x = 0$ the first order contribution to the fractal dimensions vanishes, so that only the multifractal correction term remains. Therefore the multifractal corrections completely dominate the spatial structure of the corresponding wavefunction (the most atomic one, associated to the renormalization path 00...).

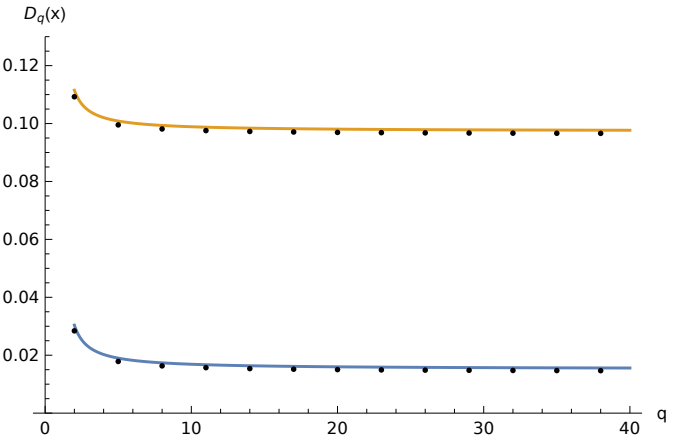

Figure 7: The fractal dimensions $D_q^\psi(x)$ of the wavefunctions for the two lowest values of x accessible numerically ($x = 0$ and $x = 1/19$ for the approximant $n = 19$ considered here). Dots are numerically computed data points, at solid lines are the theoretical predictions (eq. (31)).

To conclude this section, we show the q dependance of the fractal dimensions for fixed values of

x (fig. (7)). On the figure we show only the two lowest values of x accessible numerically, because it is for these values close to zero that the q dependance is the most visible. Again, the agreement with the theoretical predictions at the next-to-leading order is good, although we note that the theoretical values are systematically overestimating the numerical ones. This demonstrates that our theoretical analysis indeed captures the q dependance of the fractal dimensions. Since it is the multifractality of the wavefunctions that is responsible for the nontrivial q dependance of the fractal dimensions, we conclude again that the multifractal corrections are relevant even at small coupling.

Averaged wavefunction dimensions

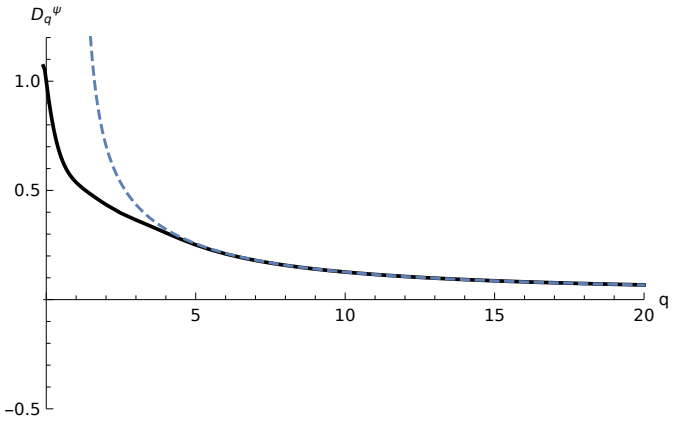

Figure 8: The averaged wavefunction dimensions D_q^ψ as a function of the multifractal parameter q. Solid line: numerical results, dashed line: theoretical predictions (eq. (33)).

Associating fractal dimensions to each individual wavefunction has given us the opportunity to study the different scaling of different wavefunctions. We have seen that to that respect the relevant parameter x. It classifies wavefunction according to their scaling, and moreover, it has a natural interpretation in the renormalization group picture. Now, we would like to characterize *globally* the wavefunctions. For that, we define an averaged fractal dimension D_q^ψ by

$$\langle \chi_q \rangle = \frac{1}{F_n} \sum_{a=1}^{F_n} \chi_q(a) \sim \left(\frac{1}{F_n} \right)^{(q-1)D_q^\psi} \tag{32}$$

This is a quantity is also frequently used in order to analyze the wavefunctions of a disordered system at the Anderson localization transition [4]. Using our perturbative Ansatz, we can easily

obtain an implicit equation on this averaged fractal dimension:

$$2\left(\frac{\lambda}{2}\right)^q \omega^{2(1-(q-1)D_q^\psi)} + \overline{\lambda}^q \omega^{3(1-(q-1)D_q^\psi)} = 1 \tag{33}$$

The authors in [9] obtained a similar relation. Contrary to theirs, our study takes into account second order corrections contained in the λ and $\overline{\lambda}$ terms. Using our explicit expression for the fractal dimensions of the wavefunctions, we can also derive an explicit expression for the averaged wavefunction dimensions TODO: do it!

We compared these theoretical predictions to numerical results on a finite size system (fig. (8)). The agreement is excellent for $q \ll 1$. This is just what we expect, as for $q < 1$ the fractal dimension probes the small components of the wavefunctions, which our analysis neglects. We note that our theoretical predictions compare much better to numerical results than the predictions of [9], who neglected the second order corrections to the wavefunctions. We conclude again that the second order corrections, which are responsible for the multifractality of the individual wavefunctions, also play a crucial role in the multifractal behavior of their average.

Local spectral dimensions and their average

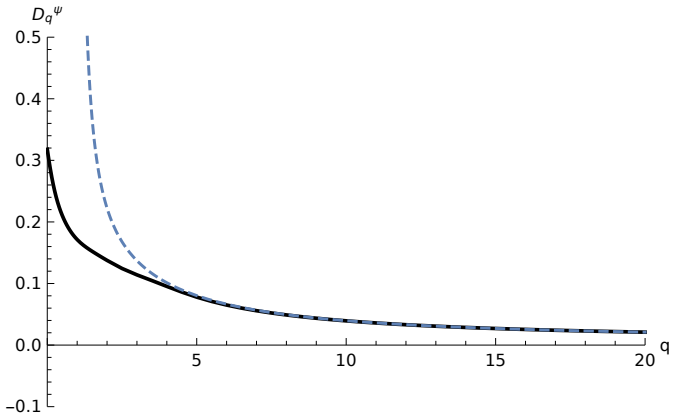

Figure 9: The averaged local spectral dimensions D_q^μ as a function of the multifractal parameter q. Solid line: numerical results, dashed line: theoretical predictions (eq. (38)).

Having characterized the spectrum and the wavefunctions in the pertubative limit, we have access to the local density of states, and in particular to the associated fractal dimensions. For a finite-size system, the local density of states at site i is just a sum of Dirac deltas:

$$\mathrm{d}\mu_i(E) = \frac{1}{F_n}\sum_{a=1}^{F_n} \delta(E - E_a)|\psi_i(a)|^2 \mathrm{d}E \tag{34}$$

Note that the sum over all sites of the local density of states is nothing but the (global) density of states. The local density of states defines μ_i, the local spectral weight at site i associated to an energy interval $[E, E']$:

$$\mu_i\left([E, E']\right) = \int_{E'' \in [E,E']} \mathrm{d}\mu_i(E'') \tag{35}$$

For the n^{th} approximant, we note $\mu_i(\Delta_a^n)$ the local spectral weight at site i associated to the a^{th} energy band. This quantity contains all the information about the spectral and wavefunction properties of the Hamiltonian. In other words, its knowledge is equivalent to the knowledge of the Hamiltonian itself. Furthermore, it has a simple physical interpretation: $\mu_i(\Delta_a^n)$ is the local density of states at site i that are in the band a. It is thus natural to probe the multifractality of the local density of states. To achieve that, we associate to each site i a gamma function

$$\Gamma^n(q, \tau; i) = \sum_a \frac{\left(\mu_i(\Delta_a^n)\right)^q}{(\Delta_a^n)^\tau} \tag{36}$$

This gamma function can be viewed as a local version of the spectral gamma function (14). Using this gamma function, we can compute the local spectral fractal dimensions. In oder to characterize the whole system, we define an averaged gamma function:

$$\langle \Gamma^n(q, \tau) \rangle = \frac{1}{F_n} \sum_i \Gamma^n(q, \tau; i) \tag{37}$$

The associate fractal dimensions, the averaged local spectral dimensions D_q^μ, obey the implicit equation:

$$2\left(\frac{\lambda}{2}\right)^q \omega^2 z^{(1-q)D_q^\mu} + \overline{\lambda}^q \omega^3 \overline{z}^{(1-q)D_q^\mu} = 1 \tag{38}$$

We compare these theoretical predictions valid in the perturbative limit with numerical data (fig. (9)). The agreement is again excellent for $q \ll 1$, as expected. It is also worth noting that D_0^μ is equal to the Hausdorff dimension, for which we have a theoretical prediction (19). The agreement is once again very good.

RELATIONS BETWEEN FRACTAL DIMENSIONS

The similarity of the relations (17), (38) and (33) giving respectively the global spectral, the local spectral and the wavefunction dimensions suggests that there might be a relation between the three. At $q = 0$, the local and global spectral dimensions coincides, and the wavefunction dimension is 1, so that we have $D_0^\mu = D_0^\psi D_0$. We find that this relations extends to any positive value of q to

$$D_q^\mu = D_q^\psi D_{1+(q-1)D_q^\psi} \tag{39}$$

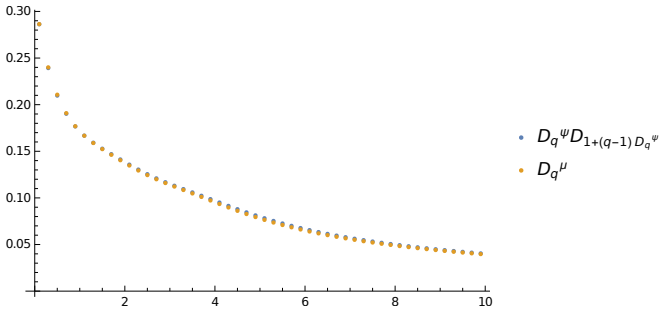

Figure 10: This plot shows the averaged local spectral dimensions superimposed with the product of the global spectral and averaged wavefunction dimensions.

Numerically (fig. (10)), the agreement is perfect. Remarkably, the relation stills holds even in the range of values of q where perturbation theory fails. These gives us hope that the relation is actually nonperturbative, and even holds for other one-dimensional models where no such perturbation theory exist. TODO: check for Fibonacci for other values of coupling, check for other cut and project chains, and investigate further the Harper case...

Renormalization factors of atomic and molecular eigenstates

In this appendix, we derive the expression of the renoralization factors λ and $\bar{\lambda}$ of the molecular and atomic eigenstates.

Atomic eigenstates

Let $|\psi(E)\rangle$ be an eigenstate for an energy E belonging to the atomic energy cluster, at step n. At first order, $|\psi(E)\rangle$ is an eigenstate of $\overline{z}H_{n-3}$, with the sites rearranged on the n^{th} approximant. Therefore, at first order $|\psi(E)\rangle$ is only nonzero on some atomic sites of the n^{th} chain. Let i label one of these sites.

The fact that $|\psi(E)\rangle$ is an eigenstate of $\overline{z}H_{n-3}$, with the sites rearranged on the n^{th} approximant translates into the equation

$$\psi_i(E) = \psi_{d_a(i)}(E/\bar{z}), \tag{40}$$

where $d_a(i)$ is the new numbering of the site i after an atomic deflation operation.

Now, at the next order, some of the intensity, that was at first order concentrated only on some atomic sites, "leaks" on the molecular sites neighbouring these atomic sites. This translates into the fact that the intensity on these atomic sites is reduced by a factor $\overline{\lambda}$. So, at second order, equation (40) becomes

$$\psi_i(E) = \sqrt{\overline{\lambda}}\psi_{d_a(i)}(E/\bar{z}). \tag{41}$$

To determine $\overline{\lambda}$, we just have to compute how much intensity has leaked out of site i.

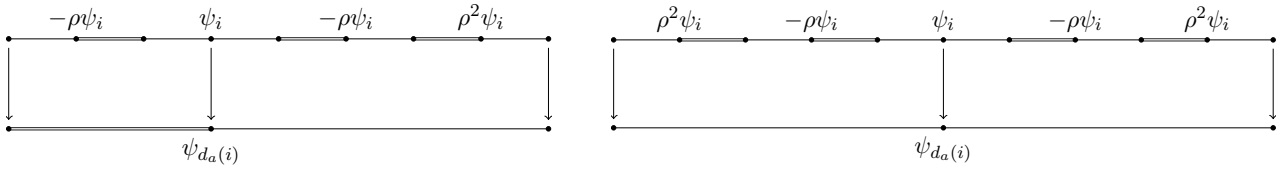

(a) Atomic site surrounded by strong and weak effective couplings.

(b) Atomic site surrounded by two weak effective couplings.

Figure 11: The two types of local environments of an atomic site.

The atomic site i we consider can either be surrounded by one weak effective bond (fig. (11a)), or by two effective weak bonds (fig. (11b)). In both cases, it is straighforward to compute, at leading order in ρ, the fraction of the amplitude at site i who is transferred to neighbouring molecular sites.

Note that destructive interferences result in half the molecular sites being unaffected at leading order.

As we already said, at first order in ρ, the amplitude in concentrated at site i. We call I the intensity at this site: $I = |\psi_i|^2$. At second order in ρ, the intensity I has spread out at neighbouring molecular sites, and therefore the intensity at site i is attenuated by a factor $\overline{\lambda}$. We have

$$\overline{\lambda} I(1 + 2\rho^2 + \mathcal{O}(\rho^4)) = I, \tag{42}$$

And thus

$$\overline{\lambda} = \frac{1}{1 + 2\rho^2} + \mathcal{O}(\rho^4). \tag{43}$$

Molecular eigenstates

[1] David Damanik and Anton Gorodetski. Spectral and quantum dynamical properties of the weakly coupled fibonacci hamiltonian. *Communications in Mathematical Physics*, 305(1):221–277, 2011.

[2] TC Halsey, MH Jensen, and LP Kadanoff. Fractal measures and their singularities: the characterization of strange sets. *Physical Review A*, 33(2), 1986.

[3] P Kalugin, A Kitaev, and L Levitov. Electron spectrum of a one-dimensional quasicrystal. *Sov. Phys. JETP*, 64(2), 1986.

[4] A D. Mirlin, Y. V. Fyodorov, A. Mildenberger, and F. Evers. Exact relations between multifractal exponents at the anderson transition. *Physical Review Letters*, 97(July):1–4, 2006.

[5] R Mosseri. Universalities in condensed matter. *Les Houches proceedings*, 42, 1988.

[6] Q Niu and Franco Nori. Spectral splitting and wave-function scaling in quasicrystalline and hierarchical structures. *Physical Review B*, 42(16), 1990.

[7] Frédéric Piéchon, Mourad Benakli, and Anuradha Jagannathan. Analytical results for scaling properties of the spectrum of the fibonacci chain. *Phys. Rev. Lett.*, 74:5248–5251, Jun 1995.

[8] C Sire and R Mosseri. Extended states, gap closing,... some exact results for codimension one quasicrystals. *J. Phys. France*, 51(15), 1990.

[9] Stefanie Thiem and Michael Schreiber. Wavefunctions, quantum diffusion, and scaling exponents in golden-mean quasiperiodic tilings. *Journal of physics. Condensed matter : an Institute of Physics journal*, 25(7):075503, 2013.